https://doi.org/10.18321/ectj1128

Study on the Rapid Preparation of Zinc Oxide Nanotubes by Galvanostatic Etching

Jingsong Sun, Jinxing Cao, Xiaohong Jiang*

Nanjing University of Science and Technology, 200, Xiaolingwei Str., Nanjing, China

Article info

Received:
10 May 2021

Received in revised form:
16 July 2021

Accepted:
24 October 2021

Keywords:
ZnO nanotubes
Galvanostatic etching
Light absorption capacity
Fluorescence properties
Dopamine test

Abstract

At present, most of the methods for preparing ZnO nanotubes are chemical etching of ZnO nanorods, which is inefficient and takes a long time. In this paper, ZnO nanotubes were successfully prepared by galvanostatic etching. Nanotubes prepared by galvanostatic etching only took 1/6 of the time of chemical etching. The ZnO nanotubes obtained by two different methods were tested by XRD and SEM. It is found that the crystal structure and crystallinity of the ZnO nanotubes obtained by galvanostatic etching are unchanged, and the internal corrosion of the nanotubes by galvanostatic etching is more thorough and has a larger specific surface area. In the tests of UV-vis spectrophotometry, fluorescence spectra and electrochemical performance test, the optical properties and electrochemical performance of ZnO nanotubes obtained by galvanostatic etching are better than those obtained by chemical etching. Because the ZnO nanotubes obtained by galvanostatic etching have larger specific surface area, better optical properties and better electrochemical performance, they have a greater application prospect in sensors and ultraviolet light detectors.

1. Introduction

ZnO is a wide band gap semiconductor, the band gap width is about 3.37 eV, the electron binding energy at room temperature is 60 meV [1], and generally presents a hexagonal wurtzite structure. ZnO semiconductor materials have good physical properties (conductivity, piezoelectricity, photoelectricity, etc.) and chemical properties (stability, gas sensitivity, etc.) [2–5], so they have widely used in optoelectronics [6], solar cells [7–8], sensors [9], field emission [10], piezoelectric [11] and catalysis [12], etc. So far, the synthesis methods of preparing ZnO nanomaterials have made great progress, mainly including the vapor deposition method [13–14], template method [15–16] and hydrothermal method [17–18]. The products synthesized by these methods have good crystallization, high purity, and controllable particle size, but these methods have more or fewer disadvantages that are difficult to overcome, such as the harsh preparation conditions of the vapor deposition method (requires high temperature, a certain gas atmosphere or high vacuum). In addition, the instrument is expensive, time-consuming to operate, the template method is less independent (need to be used with other methods), and the hydrothermal method has a long preparation cycle. Therefore, it is necessary to find a preparation method that can overcome the above disadvantages and is easy to produce on a large scale. Compared with other methods, galvanostatic deposition technology has many advantages, such as mild reaction conditions, simple equipment, high deposition rate, environmentally friendly one friendliness, and controllable morphology [19–24]. It has been widely used in the preparation of one-dimensional ZnO nanorod arrays.

Among ZnO nanomaterials, nanotubes have become a research hotspot in recent years, because nanotubes not only have a special hollow structure but also have the advantage of large surface area compared with nanorods and nanowires, which can greatly improve the application efficiency in

*Corresponding author.
E-mail: jiangxh24@njust.edu.cn

sensors, solar cells, photoelectronics and other aspects. At present, the methods of preparing ZnO nanotubes are mostly alkali chemical etching [25–27]. Although alkali chemical etching can etch ZnO nanocolumns into tubes, the etching efficiency is too low, and it takes a lot of time to completely etch to the bottom of the nanotubes. In this paper, ZnO nanotubes were prepared by galvanostatic etching for the first time. Galvanostatic corrosion can not only improve the etching effect but also greatly shorten the etching time. At the same time, the etching intensity is strong enough to directly etch the bottom of the nanotubes, thus increasing the surface area of the nanotubes to a greater extent, which can improve the optical and photoelectrochemical properties of nanotubes and get a certain improvement in the sensor, ultraviolet light detector, solar cell.

Dopamine, an important catecholamine, is a neurotransmitter [28]. All brain processes are affected by dopamine, which has a huge impact on sleep [29], memory [30], lust [31]. When the concentration of dopamine in the body is too high, dopamine harms the human body, causing Parkinson's disease, heart disease and schizophrenia. Therefore, it is necessary to detect and control the concentration of dopamine in the human body to protect human health. At present, the reported methods for detecting dopamine include fluorescence, high performance liquid chromatography [32], and chemiluminescence [33]. But these methods have the shortcoming of low sensitivity and complicated operation. An electrochemical sensor is a kind of chemical sensor that depends on electrochemical detection technology. It is widely used in the detection of chemical substances. It uses the electrode as the conversion element, the modified biomaterial on the electrode as the sensitive element to react with the analyte, and converts the received signal into an identifiable signal through the system of the electrochemical analysis device, to realize the purpose of detection. Electrochemical sensors have become one of the most important detection methods in the field of drug analysis because of their small equipment and real-time monitoring. In addition, electrochemical sensors are also used in immunoassay, biosensors and other research fields. Zinc oxide nanotubes with three-dimensional structures have a large specific surface areas, which is beneficial to ion exchange and excellent electrochemical performance. Although nanoscale zinc oxides have been improving, they have been limited in the field of electrochemical sensors due to their low electrical conductivity. In this paper, by spraying gold on the surface of zinc oxide nanotubes, the gold/zinc oxide composite material was obtained, which greatly increased the electrical conductivity of the material.

2. Materials and methods

2.1. Materials

Phosphate buffer (PBS) was acquired from Phygene Biotechnology Co Ltd. The concentration of PBS is 0.01 mol/L and the pH value of PBS is about 7.1. Zinc nitrate hexahydrate ($Zn(NO_3)_2$, hexamethylene tetramine ($C_6H_{12}N_4$) and potassium hydroxide (KOH) were purchased from Sinopharmaceuticals Chemical Reagents Co., Ltd. Dopamine hydrochloride was purchased from Suzhou Freeze Detection Technology Co., Ltd. In this experiment, the electrochemical workstation of Jiangsu Donghua Instrument Co., Ltd. (model is DH7000) and the three-electrode system are used as the test instruments. Among them, the counter electrode in the three-electrode system uses a platinum sheet, the reference electrode uses the standard Ag/AgCl electrode (filled with saturated KNO_3 solution), and the working electrode is ITO conductive glass (5 cm × 1 cm × 1 mm, resistance for 6–8 Ω).

2.2. Preparation of ZnO nanorods

First of all, 0.01mol/L zinc nitrate solution was prepared and electrodeposited with a three-electrode system for 60 s under constant potential -0.1V to prepare the ZnO seed layer, which was rinsed washed with ultra-pure water and put into the oven to dry. Then 0.02 mol/L $Zn(NO_3)_2$ and 0.02 mol/L $C_6H_{12}N_4$ were mixed to prepare 100 mL of mixed solution. The dried ZnO seed layer was deposited in a three-electrode system of 1.25 mA under constant current for 5400 s. After the deposition was completed, the prepared film was rinsed washed with ultra-pure water and put into the oven to dry to obtain ZnO nanorods.

2.3. Preparation of ZnO nanotubes by chemical etching

Weigh 2.02 g of KOH into a beaker, add 100 mL of ultra-pure water, and stir well. Then, the prepared ZnO nanorods were placed in potassium hydroxide solution and etched in a water bath at 80 °C for 60 min. The obtained sample is rinsed with ethanol and put into the oven to dry.

2.4. Preparation of ZnO nanotubes by galvanostatic etching

Weigh 2.02 g of KOH into a beaker and add 100 mL of ultra-pure water to make a solution. The prepared ZnO nanorods were placed in the solution and etched at 20 mA constant current for 10 min using the three-electrode system. The etched samples were washed clean with ethanol and dried in the oven.

2.5. Preparation of gold/zinc oxide composites

The gold was sprayed on the ZnO nanoarray with a gold spray apparatus, the gold spraying time was 120 s, the current size was 2 mA, the gold/ZnO nanorods were obtained, and the gold/ZnO nanotubes were obtained by two different methods.

2.6. Characterizations

The composition and crystal structure of the samples were analyzed by X-ray diffraction (XRD, Brook D8 Advance). The diffractometer's radiation source used a Cu target, which was intended to set the voltage and current inside the tube to 40 kV and 20 mA respectively, with a scanning range of 20° to 80°.

Scanning electron microscopy (SEM, FEI Quanta 250FEG) was used to characterize the microscopic morphology of the samples. Because our samples are semiconductors and have conductivity itself, it is not necessary to spray gold before testing. FL3-TCSPC fluorescent spectrometer was used for the fluorescence spectrum analysis of ZnO samples. The excitation wavelength was 325 nm, and the measured wavelength range was 350–600 nm.

UV-Vis spectrophotometer (UV-Vis, Perkin-Elmer Lambda 950) was used to measure the light absorption capacity of the sample in a certain band and the test results against the background of barium sulfate were used as the standard baseline. During the test, the surface baseline was first scanned, and then the sample was placed on the barium sulfate substrate for scanning at a wavelength range of 300–600 nm.

2.7. Electrochemical test

The electrochemical performance of the sensor was tested through the electrochemical workstation provided by Donghua Instrument Company, which includes electrochemical impedance spectroscopy (EIS) and differential pulse voltammetry (DPV). EIS was performed on the sample in a potassium chloride solution to investigate the resistance and charge transfer rate of the sample. Before the EIS test, the open circuit potential of the sample was measured and the frequency speed was set at 1 ~ 100000 Hz. As for DPV, the main parameters are set as follows: pulse width is 60 ms, the amplitude is 50 mV, sweep potential range is −0.15V~0.45V.

3. Results and discussion

3.1. X-ray diffraction analysis

Figure 1 shows the X-ray diffraction patterns of ZnO nanorods, ZnO nanotubes etched by chemical etching and ZnO nanotubes prepared by galvanostatic etching. It is not hard to see from the picture, there are several characteristics of diffraction peak, at 31.8° and 34.4° and 36.2° and 62.9°on the ZnO samples, respectively corresponding crystal face (100), (002), (101), (103), and all of the angle and intensity peak with the standard PDF (JCPDS: 36-1451) card is consistent, and with the six-party reported in the literature of the ZnO diffraction peak corresponding to [36]. This indicates that we have successfully prepared ZnO nanorod arrays and nanotube arrays with hexagonal wurtzite structures. At the position of 2θ about 34.4°, corresponding to the crystal plane of (002), there is a ZnO diffraction peak with the strongest intensity, which is higher than other diffraction peaks, and the half-width peak is the smallest. It means that the ZnO of the two prepared structures have the best orientation here, which is in accordance with the ZnO nanoarray growing perpendicular to the conductive glass in the SEM figure below. In addition, there are no other heteropeaks in the X-ray diffraction pattern, which indicates that the prepared ZnO nanomaterials have high purity and crystallinity.

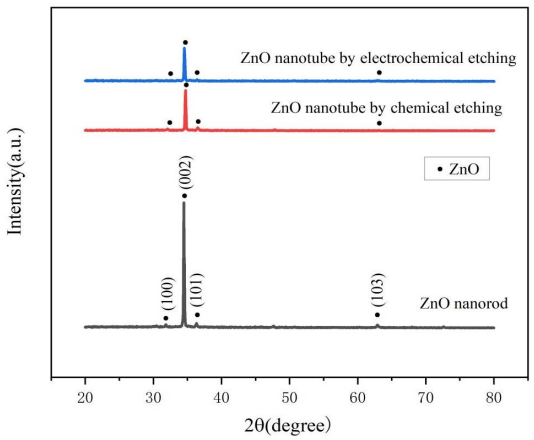

Fig. 1. X-ray diffraction analysis of two kinds of ZnO nanostructures.

Compared with ZnO nanorods, the peak position and strength of ZnO nanotubes prepared by chemical etching and galvanostatic etching are unchanged, indicating that the prepared ZnO nanotubes have the same hexagonal wurtzite structure as the nanorods, and have high purity and crystallinity.

3.2. Microstructure analysis

Figure 2 is shown are scanning electron microscopy images of ZnO nanorods, ZnO nanotubes by chemical etching, and ZnO nanotubes by galvanostatic etching respectively. According to the overall morphology of ZnO nanorods, the ZnO nanorods prepared in this experiment grow uniformly and neatly perpendicular to the substrate. Moreover, ZnO nanorods have regular hexagonal morphology, with smooth surfaces and sides. The diameter of nanorods is about 500 nm. The inner diameter of ZnO nanotubes prepared by chemical etching is about 250 nm, and the wall thickness is about 125 nm. The inner diameter of ZnO nanotubes prepared by chemical corrosion is about 250 nm and the wall thickness is about 125 nm. In contrast, the ZnO nanotubes prepared by galvanostatic etching have an inner diameter of about 300 nm and a wall thickness of about 100 nm. The inner diameter of ZnO nanotubes prepared by galvanostatic etching is slightly larger than that of nanotubes prepared by chemical etching. At the same time, it can be seen from the SEM picture that the diameter of the nozzle position of the ZnO nanotubes obtained by chemical etching is larger than that of the inside of the tube, while the ZnO nanotubes obtained by electrochemical etching are almost the same from top to bottom. Therefore, the structure and specific surface area of ZnO nanotubes obtained by electrochemical etching are better than those obtained by chemical etching.

The ZnO nanorod array is etched into a nanotube array at a certain temperature, rather than the entire rod body being etched. The reason is that the axis position of the ZnO nanorod array is relatively weak and preferentially has an etched position. Since no auxiliary reagent is added in the solution, the phenomenon that the axis position of the nanorods is preferentially corroded is related to the characteristics of the ZnO nanorods. First of all, the {0001} plane of ZnO hexagonal prism nanorods have high surface energy and is metastable, so etching will preferentially start from the metastable surface of ZnO. Secondly, there are many defects in the axis of the zinc oxide hexagonal prism nanorods, which makes it easy to be etched [34]. After energizing, the following reactions take place in the electrolyte. The anode ZnO reacts with OH^-, loses two electrons and obtains ZnO_2^{2-} and oxygen at the same time. The metastable surface at the center of the ZnO hexagonal prism nanorods is the priority for etching. The water at the cathode is gaining four electrons, forming OH^- and hydrogen. The specific equation is as follows:

$$2ZnO - 4e^- + 8OH^- \rightarrow 2ZnO_2^{2-} + 4H_2O + O_2$$

$$4H_2O + 4e^- \rightarrow 4OH^- + 2H_2$$

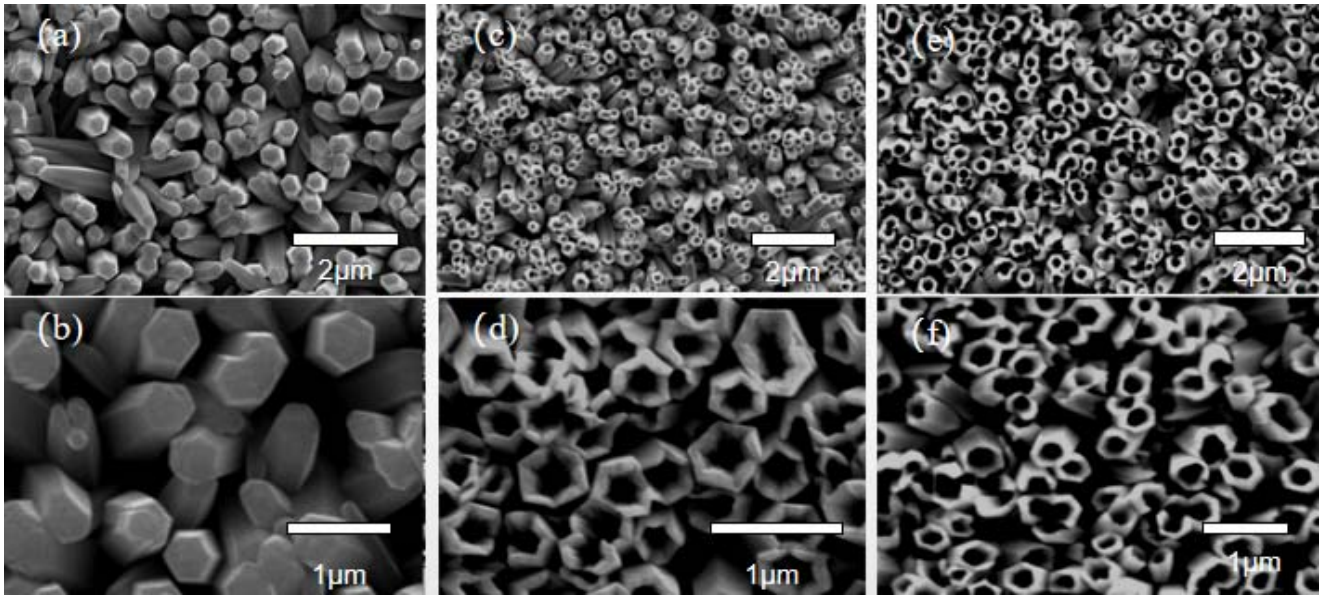

Fig. 2. Scanning electron microscope images of ZnOs with different structures: (a-b) is ZnO nanorods; (c-d) is ZnO nanotubes by chemical etching; (e-f) is ZnO nanotubes by galvanostatic etching.

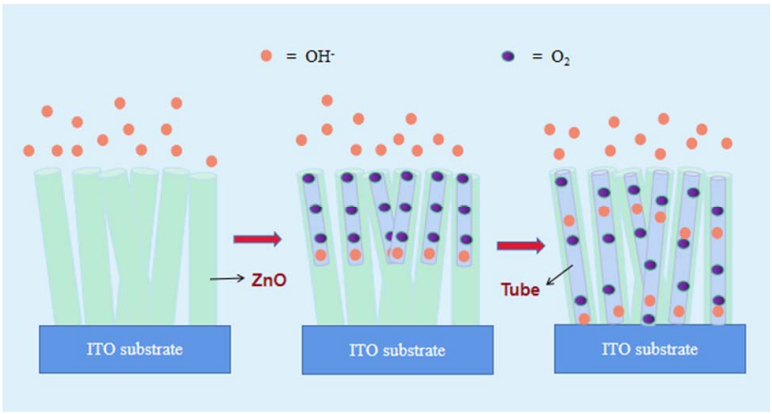

Fig. 3. Schematic diagram of the preparation of ZnO nanotubes by galvanostatic etching.

The general equation is as follows:

$$2ZnO + 4OH^- \rightarrow 2ZnO_2^{2-} + 2H_2 + O_2$$

Under the action of the current, the anode ZnO and OH^- in the solution react quickly, and the cathode generates hydroxide ions at the same time. Then the OH^- ions flow to the anode continuously and continue to react with ZnO, accelerating the etching of ZnO metastable surface. The schematic diagram of the reaction principle of the working electrode is shown in Fig. 3.

3.3. Fluorescence spectral analysis

Fluorescence spectra of the three samples are shown in Fig. 4. The ultraviolet emission peak of ZnO nanorods appears at 380 nm, while the fluorescence intensity of the nanotubes increased and the emission wavelength in the ultraviolet region shifted to about 392 nm. The reason why the fluorescence intensity of ZnO nanotubes is higher than that of nanorods is that ZnO nanotubes have a larger specific surface area, which can absorb more ultraviolet light and emit stronger fluorescence. It can be seen from the figure that the fluorescence intensity of ZnO nanotubes obtained by galvanostatic corrosion is stronger than that obtained by chemical corrosion, which proves from the side that the nanotubes obtained by galvanostatic corrosion have a larger specific surface area. Ultraviolet excitation is are commonly referred to as the near band edge emission, is due to the annihilation of the excitons, namely exciton and exciton occurred in the process of collision gets free exciton reorganization to the light. In addition, the visible emission band, between 450 and 600 nm is known as defect-related emission [35]. The three samples

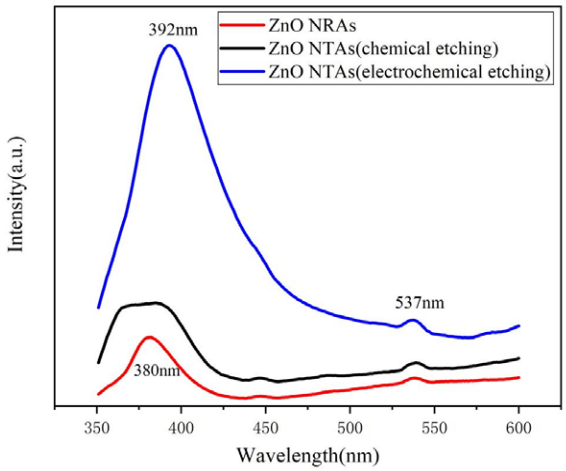

Fig. 4. Fluorescence spectra of ZnOs with different structures.

all have a weak green light emission peak in the visible region, with a central wavelength of about 537 nm, which is caused by the internal defects of ZnO. The crystal defects induced energy levels within the bandgap of ZnO allows the emission of visible light after relaxation of electron-hole pairs in the ground state.

3.4. UV–vis spectrophotometry

The UV-Vis images of ZnO with two different nanostructures are shown in Fig. 5. It can be seen from Fig. 5 that both of the two nanostructures of ZnO have a certain light absorption capacity in the ultraviolet region, and their UV absorption band is in the range of 300–380 nm, while their light absorption capacity is weak in the visible region. By comparing the ultraviolet absorbance regions of ZnO nanorods and nanotubes, ZnO nanotubes have better light absorption ability in the ultraviolet region than ZnO nanorods, because ZnO nanotubes had a larger specific surface area, their light

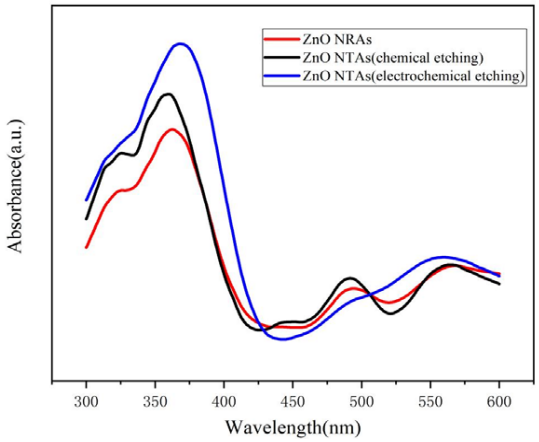

Fig. 5. UV-Vis absorption spectroscopy of ZnOs with different structures.

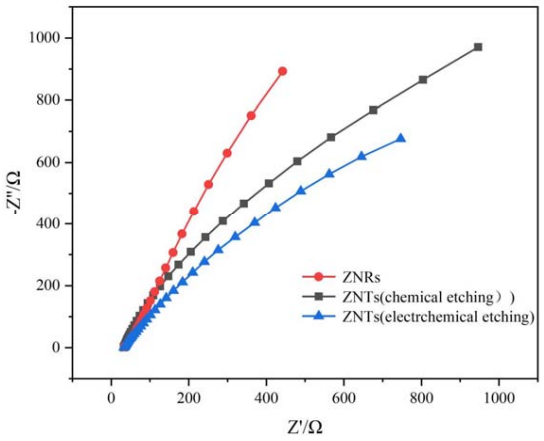

Fig. 6. EIS of Au/ZnO nanoroad, Au/ZnO nanotube by chemical etching, Au/ZnO nanotube by electrochemical etching.

absorption ability was also stronger. Comparing the two different etching methods of ZnO nanotubes light absorption ability, the photoabsorption of ZnO nanotubes by galvanostatic etching is better than that of alkali-etched ZnO nanotubes in the ultraviolet region. It is also reflected from the side that alkali etching strength is insufficient, chemical corrosion of ZnO nanotubes and galvanostatic corrosion of ZnO nanotubes etching effect is better, and has a more specific surface area.

3.5 Electrochemical test

In order to improve the electrical conductivity of the sensor, a layer of gold was sprayed on the zinc oxide substrate. EIS test was performed on the gold-sprayed zinc oxide, as shown in Fig. 6. The semicircular of the sample test curve in EIS directly reflects the charge transfer resistance, and the smaller the semicircular arc radius is, the smaller the charge transfer resistance of the corresponding sample is. From the Fig. 6, it can be found that the semi-circular arc radius of Au/ZnO nanorods is significantly larger than that of Au/ZnO nanotubes, which indicates that the charge transfer resistance of Au/ZnO nanotubes is significantly smaller than that of Au/ZnO nanorods. The semi-arc radius of the galvanostatic etched Au/ZnO nanotubes is smaller than that of the chemically etched Au/ZnO nanotubes, indicating that the charge transfer resistance of the galvanostatic etched nanotubes is smaller than that of the nanotubes by chemical etching.

Figure 7 shows the DPV test of different concentrations of dopamine hydrochloride by Au/ZnO nanorods, Au/ZnO nanotubes prepared by chemical etching and Au/ZnO nanotubes etched by constant current. The concentration of dopamine hydrochloride was 0.1 μM, 0.5 μM, 1 μM, 2 μM, 4 μM, 8 μM, 10 μM, 20 μM, 50 μM, and 100 μM respectively. Compared with ZnO nanorods, ZnO nanotubes have lower charge transfer resistance, and the sensitivity of Au/ZnO nanotubes electrodes to dopamine is about 2.1~3.4 times higher than that of Au/ZnO nanorods. Figure 7 (A), (C) and (E) shows the DPV test of Au/ZnO nanorod electrode, Au/ZnO nanotube electrode prepared by chemical etching and Au/ZnO nanotube electrode prepared by galvanostatic etching in 0.1–100 μM dopamine hydrochloride. As can be seen from the figure, the characteristic peak of Au/ZnO electrode has a peak at about 0.7 V. Figure 7(B), (D) and (F) show the linear relationship between dopamine concentration and peak DPV current of Au/ZnO electrode. As can be seen from the figure, when the concentration of dopamine hydrochloride is between 0.1–10 μM, there is a linear relationship between the concentration and the peak current. When the concentration is between 10–100 μM, there is another linear relationship between the concentration and the peak current. The specific equations are shown in the figure. The slope of these lines is the sensitivity of the sensor. Obviously, the sensitivity of the nanotube electrode is much higher than that of the nanorod electrode, because nanotubes have better electrical conductivity. At the same time, the sensitivity of the electrodes prepared by galvanostatic etching is higher than that prepared by chemical etching, which also shows that the specific surface area of the ZnO nanotubes prepared by galvanostatic etching is larger than that of the nanotubes

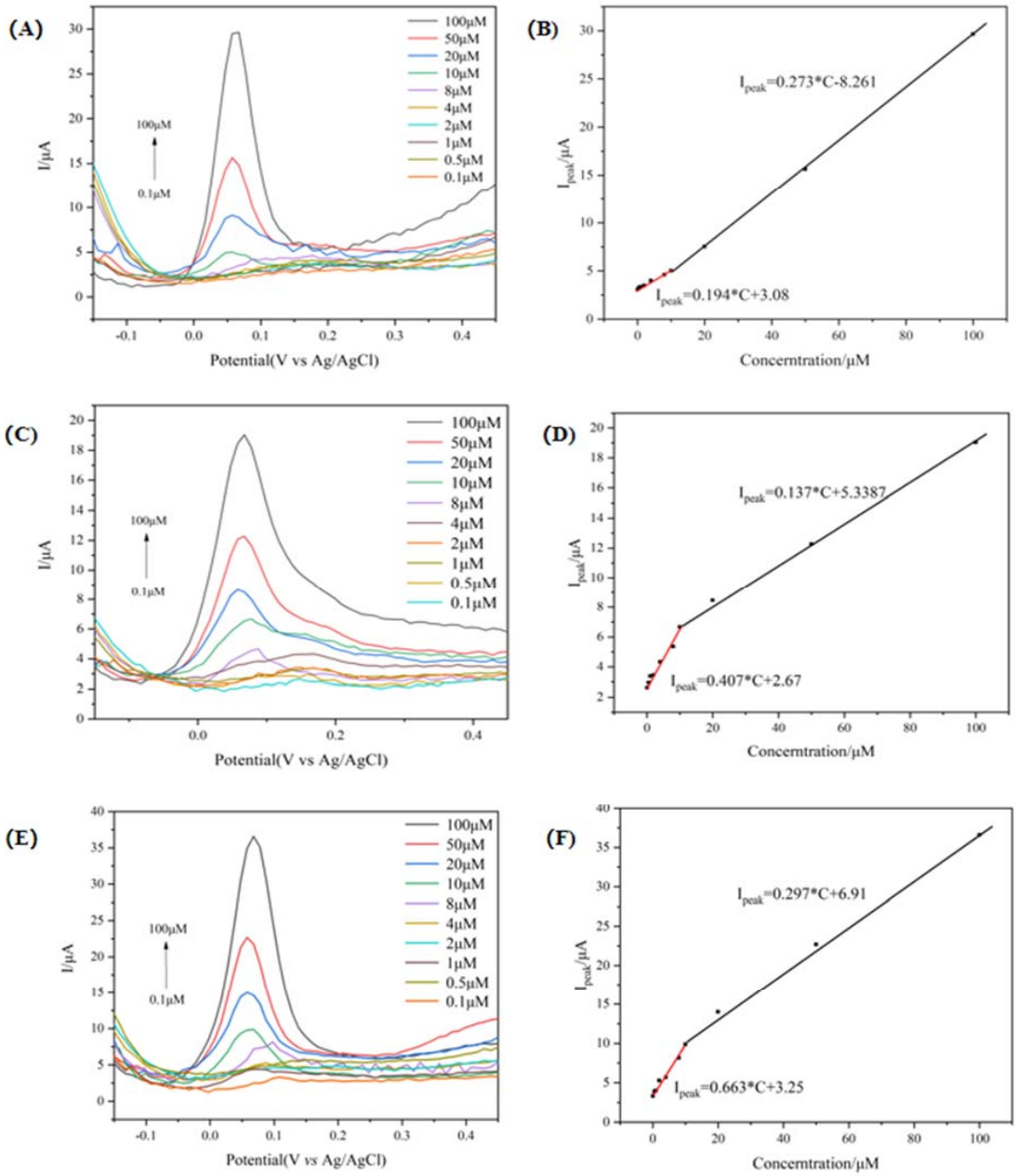

Fig. 7. (A) – DPV test of Au/ZnO nanorods in different concentrations of dopamine hydrochloride solution (B) – Linear diagram of the DPV oxidation peak current of Au/ZnO nanorods in different concentrations of dopamine hydrochloride solutions (C) – DPV test of Au/ZnO nanotubes by chemical etching in different concentrations of dopamine hydrochloride solution (D) – Linear diagram of the DPV oxidation peak current of Au/ZnO nanotubes by chemical etching in different concentrations of dopamine hydrochloride solutions (E) – DPV test of Au/ZnO nanotubes by electrochemical etching in different concentrations of dopamine hydrochloride solution (F) – Linear diagram of the DPV oxidation peak current of Au/ZnO nanotubes by electrochemical etching in different concentrations of dopamine hydrochloride solutions.

prepared by chemical etching, and the electrical conductivity of the ZnO nanotubes prepared by galvanostatic etching is better.

4. Conclusion

This article uses the galvanostatic etching method to prepare zinc oxide nanotubes for the first time. The obtained ZnO nanostructures are hexagonal prisms with hexagonal crystal structure, neatly arranged, the diameter of the nanotubes is about 500 nm, and the diameter of the tube is about 300 nm. Optical performance tests show that, compared with zinc oxide nanotubes obtained by chemical etching, nanotubes obtained by galvanostatic corrosion have better absorption and fluorescence

properties in the ultraviolet region because of their larger specific surface area. The charge transfer resistance of the ZnO nanotube array is smaller than that of the ZnO nanorod array, and the charge transfer resistance of the nanotube array obtained by constant current etching is lower than that of the nanotube obtained by chemical etching. It can be shown that the zinc oxide nanotubes obtained by constant current etching have higher charge separation and transfer efficiency, can effectively reduce the charge transfer resistance of the electrode. The DPV of dopamine hydrochloride proves that zinc oxide can be successfully applied to the sensor field, and the sensitivity of the nanotubes is better than that of the nanorods. The sensitivity of the galvanostatic zinc oxide nanotubes is better than that of the chemically etched nanotubes. Because of its better optical performance and photoelectrochemical performance, ZnO prepared by constant current etching has great application prospects in sensors, ultraviolet light detectors, and solar panels.

Acknowledgements

Ministry of Science and Technology of the People's Republic of China (No. 2016YFE0111800), and Nanjing University of Science & Technology Independent Research Project (No. 30919013301).

References

[1]. Y. Chen, D.M. Bagnall, H.J. Koh, K. Park, K. Hiraga, Z. Zhu, T. Yao, *J. Appl. Phys.* 84 (1998) 3912–3918. DOI: 10.1063/1.368595

[2]. Z.C. Tu, X. Hu, *Phys. Rev. B* 74 (2006) 035434. DOI: 10.1103/PhysRevB.74.035434

[3]. A. Kmita, B. Hutera, E. Olejnik, A. Janas. Effect of water glass modification with nanoparticles of zinc oxide on selected physical and chemical properties of binder and mechanical properties of sand mixture. *Archives of Foundry Engineering* 12 (2012) 37–40.

[4]. H. Yin, V.A. Coleman, P.S. Casey, B. Angel, H.J. Catchpoole, L. Waddington, M.J. McCall, *J. Nanopart. Res.* 17 (2015) 96. DOI: 10.1007/s11051-014-2851-y

[5]. H.A. Depew, *Rubber Chem. Technol.* 14 (1971) 259–272. DOI: 10.5254/1.3540016

[6]. M. Ollinger, Nano-encapuslated of zinc sulfide:silver with indium tin oxide and aluminum doped zinc oxide for flat panel display applications. Thesis (Ph.D.) – University of Florida, 2002. Publication Number: AAI3084028.

[7]. N. Wolf, T. Stubhan, J. Manara, V. Dyakonova C.J. Brabecbc, *Thin Solid Films* 564 (2014) 213–217. DOI: 10.1016/j.tsf.2014.06.008

[8]. J. Deng, M. Wang, Z. Yang, J. Liu Z. Sun, X. Song, *J. Power Sources* 280 (2015) 555–564. DOI: 10.1016/j.jpowsour.2015.01.137

[9]. R. Badry, A. Fahmy, A. Ibrahim, H. Elhaes, M. Ibrahim, *Opt. Quant. Electron.* 53 (2021) 39. DOI: 10.1007/s11082-020-02646-5

[10]. R.C. Pawar, J.W. Lee, V.B. Patil, C.S. Lee, *Sensor. Actuat. B-Chem.* 187 (2013) 323–330. DOI: 10.1016/j.snb.2012.11.100

[11]. G. Ferblantier, F. Mailly, R.A. Asmar, A. Foucaran, F. Pascal-Delannoy, *Sensor. Actuat. A-Phys.* 122 (2005) 184–188. DOI: 10.1016/j.sna.2005.04.009

[12]. A. Wittmar, D. Gautam, C. Schilling, U. Dörfler, W. Mayer-Zaika, M. Winterer, M. Ulbricht, *J. Nanopart. Res.* 16 (2014) 2341. DOI: 10.1007/s11051-014-2341-2

[13]. J. Nishino, Y. Nosaka, *J. Cryst. Growth* 268 (2004) 174–177. DOI: 10.1016/j.jcrysgro.2004.05.006

[14]. X.H. Wang, L.Q. Huang, L.J. Niu, R.B. Li, D.H.Fan, F.B. Zhang, Z.W. Chen, X. Wang, Q.X. Guo, *J. Alloy. Compd.* 622 (2015) 440–445. DOI: 10.1016/j.jallcom.2014.10.077

[15]. A. El Mragui, I. Daou, O. Zegaoui, *Catal. Today* 321–322 (2018) 41–51. DOI: 10.1016/j.cattod.2018.01.016

[16]. Y. Kokubun, H. Kimura, S. Nakagomi, *Jpn. J. Appl. Phys.* 42 (2003) L904–L906. DOI: 10.1143/JJAP.42.L904

[17]. T.S. Perundevi, A. Karthika, S. Ramalakshmi *Mater. Today: Proc.*, 2021. DOI: 10.1016/j.matpr.2020.11.721

[18]. M.H. Farooq, R. Hussain, M.Z. Iqbal, M.W. Shah, U.A. Rana, S.U-D. Khan, *J. Nanosci. Nanotechno.* 16 (2016) 898–902. DOI: 10.1166/jnn.2016.10705

[19]. R. Zakerian, S. Bahar, *J. Sep. Sci*. 40 (2017) 4439–4445. DOI: 10.1002/jssc.201700799

[20]. D. Dimova-Malnovska, P. Andreev, M. Sendova-Vassileva, H. Nichev, K. Starbova, *Energy Procedia* 2 (2010) 55–58. DOI: 10.1016/j.egypro.2010.07.010

[21]. H. Haga, M. Jinnai, S. Ogawa, T. Kuroda, Y. Kato, H. Ishizaki, *Electr. Eng. Japan* 140 (2021) 357–363. DOI: 10.1002/eej.23320

[22]. R. Sang, Y. Zhang, J. Shao, C. Yan, K. Zhao, *J. Alloy. Compd*. 777 (2019) 506–513. DOI: 10.1016/j.jallcom.2018.10.407

[23]. T. Wen, H. Tan, S. Chen, P. He, S. Yang, C. Deng, S. Liu, *Electrochem. Commun.* 128 (2021) 107073. DOI: 10.1016/j.elecom.2021.107073

[24]. Y.-L. Xie, J. Yuan, P Song, S-Q. Hu, *J. Mater. Sci: Mater. Electron.* 26 (2015) 3868–3873. DOI: 10.1007/s10854-015-2913-7

[25]. J. Chen, Y. Jia, W. Wang, J. Fu, H. Shi, Y. Liang, *Int. J. Hydrogen Energ.* 45 (2020) 8649–8658. DOI: 10.1016/j.ijhydene.2020.01.114
[26]. M. Yousefi, M. Amiri, R. Azimirad, A.Z. Moshfeghad, *J. Electroanal. Chem.* 661 (2011) 106–112. DOI: 10.1016/j.jelechem.2011.07.022
[27]. X. Gan, X. Li, X. Gao, W. Yu, *J. Alloy. Compd.* 481 (2009) 397–401. DOI: 10.1016/j.jallcom.2009.03.013
[28]. P.C. Pandey, A.K. Pandey, *Electrochim. Acta* 109 (2013) 536–545. DOI: 10.1016/j.electacta.2013.07.142
[29]. J.M. Monti, D. Monti, *Sleep Med. Rev.* 11 (2007) 113–133. DOI: 10.1016/j.smrv.2006.08.003
[30]. T.S. Tang, X. Chen, J. Liu, I. Bezprozvanny, *J. Neurosci.* 27 (2007) 7899–7910. DOI: 10.1523/JNEUROSCI.1396-07.2007
[31]. M.K. Lakshmana, T.R. Raju, *Anal. Biochem.* 246 (1997) 166–170. DOI: 10.1006/abio.1996.9997
[32]. O. Szerkus, J. Jacyna, P. Wiczling, A. Gibas, M. Sieczkowski, D. Siluk, M. Matuszewski, R. Kaliszana, M.J. Markuszewskia, *J. Chromatogr. B* 1029–1030 (2016) 48–59. DOI: 10.1016/j.jchromb.2016.06.051
[33]. Y. Liu, X. Huang, J. Ren, *Electrophoresis* 37 (2016) 2–18. DOI: 10.1002/elps.201500314
[34]. J. Yang, Y. Lin, Y. Meng, Y. Liu, *Ceram. Int.* 38 (2012) 4555–4559. DOI: 10.1016/j.ceramint.2012.02.033
[35]. M. Willander, O. Nur, J.R. Sadaf, M.I. Qadir, S. Zaman, A. Zainelabdin, N. Bano, I. Hussain, *Materials* 3 (2010) 2643–2667. DOI: 10.3390/ma3042643
[36]. P.Y. Kuang, Y.Z. Su, K. Xiao, Z.-Q. Liu, N. Li, H.-J. Wang, J. Zhang, *ACS Appl. Mater. Interfaces* 7 (2015) 16387–16394. DOI: 10.1021/acsami.5b03527